Argo — Two Decades: Global Oceanography, Revolutionized

24 February 2021

submitted to: *Annual Reviews of Marine Science 2021*

Gregory C. Johnson, NOAA/Pacific Marine Environmental Laboratory, Seattle WA, USA gregory.c.johnson@noaa.gov

Shigeki Hosoda, Japan Agency for Marine-Earth Science and Technology, Kanagawa, Japan hosodas@jamstec.go.jp

Steve Jayne, Woods Hole Oceanographic Institution, Woods Hole MA, USA sjayne@whoi.edu

Peter R. Oke, CSIRO Marine and Atmospheric Research, Hobart TAS, Australia peter.oke@csiro.au

Stephen C. Riser, University of Washington, Seattle WA, USA riser@uw.edu

Dean Roemmich, Scripps Institution of Oceanography, La Jolla CA, USA droemmich@ucsd.edu

Tohsio Suga, Tohoku University, Sendai, Japan suga@tohoku.ac.jp

Virginie Thierry, Ifremer, Brest, France vthierry@ifremer.fr

Susan E. Wijffels, Woods Hole Oceanographic Institution, Woods Hole MA, USA swijffels@whoi.edu

Jianping Xu, Second Institute of Oceanography, Hangzhou, China sioxjp@139.com

Shortened running title: Argo — Two Decades: Global Oceanography, Revolutionized

Corresponding author: Gregory C. Johnson, NOAA/Pacific Marine Environmental Laboratory, 7600 Sand Point Way NE Bldg. 3, Seattle WA 98115 USA, gregory.c.johnson@noaa.gov

Table of Contents

Key Words
Anthropogenic climate change
Ocean variability
Ocean physics
Weather prediction
Ocean reanalysis

Abstract

Argo, an international, global observational array of autonomous robotic profiling floats nearly 4000-strong, each measuring ocean temperature and salinity from 0–2000 m on nominal 10-day cycles, has revolutionized physical oceanography. Argo started at the turn of the millennium, growing out of advances in float technology over the previous several decades. After two decades, with well over 2 million profiles made publicly available in real-time, Argo data have underpinned more than 4000 scientific publications and improved countless nowcasts, forecasts, and projections. We review a small subset of those accomplishments such as elucidation of remarkable zonal jets spanning the deep tropical Pacific; increasing understanding of ocean eddies and mixing roles in shaping water masses and circulation; illuminating interannual to decadal ocean variability; quantifying, in concert with satellite data, contributions of ocean warming and ice melting to sea level rise; improving coupled numerical weather predictions; and underpinning decadal climate forecasts.

1. Introduction

Argo, an international scientific program begun in 1999, measures seawater properties and circulation of the subsurface ocean using autonomous profiling floats. It has been successful and influential, enabling over 4000 scientific publications since its inception. The New York Times (Gillis 2014) referred to Argo as "…one of the scientific triumphs of the age…". Argo is motivated by the central roles of the ocean in Earth's climate. Oceans cover over 70% of the planet's surface and contain over 95% of its water. The land (relatively immovable) and the atmosphere (with relatively low heat capacity) also play important roles in Earth's climate, but the ocean's massive heat capacity, global circulation, and thermal inertia are key.

Accurate quantitative assessments of the ocean's roles in climate require continuous and global observations to define the ocean state and reveal its full complexity. Prior to Argo, however, vast expanses of the world ocean, especially below the surface, were largely inaccessible. One of the earliest documented sets of useful ocean measurements was made by Benjamin Franklin around 1770. He used observations of ocean temperature made on voyages between Europe and the English colonies to determine the structure and path of the Gulf Stream (Folger 1787). A hundred years later, the *Challenger* expedition (1872–76) vastly increased the database by completing the first systematic survey of the world ocean, collecting ship-based measurements of temperature to depths as great as several thousand meters at more than 250 sites in the Atlantic, Pacific, and Indian oceans (Wyville-Thompson & Murray 1885).

Over the ensuing century, vessel and measurement technology continued to improve, and dedicated oceanographic laboratories with seagoing capabilities were founded. By the 1980s oceanographers had gathered a nascent, global data set consisting of a few thousand high-quality stations with full-depth temperature and salinity measurements, with a considerably smaller concomitant biogeochemical data set, and some early transient tracer observations. Analyses of these data illuminated a global, 3-dimensional circulation composed of localized, deep sinking of water at high latitudes in the North Atlantic and around Antarctica, compensated by slow upwelling in the deep sea over the rest of the world ocean. This was all connected by deep flows away from the sinking regions and shallower return circulations. Such a global scenario had been hypothesized previously (Stommel 1957), and analyses of the data extant circa 1980 confirmed the idea (Warren 1981).

By the early 1980s oceanographers also realized that, despite increases in the global observational database and gains in our understanding of some aspects of the large-scale circulation, most of the subsurface ocean had still never been surveyed. The ambitious World Ocean Circulation Experiment (WOCE) was conceived to remedy this situation with a ship-based survey of the world ocean, covering all the main basins and sub-basins at several thousand sites. Over 4000 new full-ocean-depth stations, sampling a wide range of physical and chemical parameters, were occupied as part of WOCE (King et al. 2001). More than a decade was required to complete this survey, and even now, several decades later, the data in the WOCE archive comprise an incomparable reference dataset, and their analysis continues.

An additional component of WOCE was the deployment of a newly-developed instrument, the Autonomous Lagrangian Circulation Explorer, or ALACE (Davis et al. 1992). ALACE was a freely-drifting float that spent most of its time at a depth of 1000 m and ascended to the sea surface for a few hours to transmit its location via satellite at intervals of roughly 10 days, then descended back to 1000 m for another 10 days. Its ascent and descent were controlled by the inflation and deflation of an external oil bladder. Differencing the positions between adjacent 10-day cycles yields estimates of the 10-day average velocity vector at 1000 dbar. Hundreds of ALACE floats were deployed throughout the world ocean during WOCE. The resulting pioneering velocity dataset (Davis 2005) provided the first-ever global view of the large-scale absolute velocity field in the deep sea. The beauty of ALACE was its simplicity: The floats were relatively inexpensive, no dedicated ship time was required for deployment or recovery, and the position data were available in near real-time. The floats were capable of unattended operation for several years. Towards the end of WOCE, in the mid-1990s, a subset of ALACE floats was equipped with sensors to measure temperature at selected pressures during each ascent that were transmitted by satellite along with float positions (Kwon & Riser 2004). By the end of the decade some ALACE-type floats had been equipped with CTD instruments (Lavender et al. 2000).

While ship-based surveys over the past century were useful for exploring the sub-surface ocean state, they were all one-time efforts with large gaps between ship-tracks. By the late 1990s, the question of climate change and the ocean's roles in it was becoming a central issue. Providing answers and developing useful climate models required an examination of the time-dependent state of the global ocean. Repeating vessel-based WOCE-type sampling at the temporal and

spatial scales required was not practical: Ships were expensive, and there were too few of them. However, making CTD measurements at hundreds or even thousands of locations in the world ocean at regular intervals from autonomous platforms seemed worth considering.

Informal musings of possibilities of an array of ALACE-type instruments equipped with CTD instruments (which by then had become known as profiling floats) gave way to more formal discussions among groups of oceanographers, engineers, and program managers. By 1999 an implementation plan for what became known as Argo had emerged (Argo Science Team 1998). It called for a global array of roughly 3000 CTD-equipped profiling floats profiling to 2000 m at 10-day intervals, deployed at roughly 300 km intervals throughout the ice-free regions of the world ocean. Further, it was stipulated that the data transmitted by the floats should be made freely available in real-time over the rapidly developing internet.

The quantity of instrumentation, the global coverage, and the real-time, free availability of data were each forward-looking concepts; when considered together, the plan for Argo was revolutionary. The proposal for Argo was soon endorsed by the World Meteorological Organization as part of the Global Ocean Observing System. The first Argo float deployments took place in 1999, with the pace of deployments rapidly accelerating. An internet-based system to archive the data, make them available in real-time, and provide a corrected version six months to a year later, was created from scratch over the course of several years; a major milestone in itself that still operates today (Wong et al. 2020). By 2007 the Argo array consisted of 3000 floats, by 2012 over 1 million profiles were available in the Argo global archive (Riser et al.

2016), the 2 millionth profile was collected in 2018, and by 2020 the array was approaching 4000 floats, with some models profiling to full depth and others equipped with biogeochemical sensors. The quality and increasing quantity of Argo data over the past two decades have lived up to the revolutionary vision (Figure 1). Some examples of the advancements made possible by Argo follow.

2. Illuminating the Depths with Improved Ocean Climatologies

For the first time, Argo has allowed construction of contemporaneous observational global ocean climatologies of temperature, salinity, and velocity from the sea surface to 2000 m, including the mean and seasonal cycle. In contrast, most pre-Argo climatologies were blended, from sparser, spatially and temporally inhomogeneous data heavily biased towards particular regions, seasons, and years. Argo-era climatologies have shed substantial light on many previously obscure or undiscovered ocean features worldwide.

2.1 The Mean Circulation and Water-Mass Properties

Owing to their spatially and temporally unbiased sampling and high-quality near-global coverage, Argo data alone allow realistic three-dimensional monthly climatologies of temperature and salinity of the modern, or Argo-era from 0 to 2000 m through objective analysis on isobaric surfaces (e.g., Roemmich & Gilson 2009). More elaborate Argo-based products refine further the picture of the oceanic mean state: For example, by providing statistics and preserving the time and space sampling capability of Argo (e.g., Gaillard et al. 2016), or by mapping on isopycnal surfaces with consideration of fronts and bathymetry (e.g., Schmidtko et

al. 2013). Existing global full-depth climatologies have also been updated with Argo data (e.g., Gouretski 2019).

Innovative analyses of Argo data have improved our picture of upper ocean structure. For example, a new algorithm to detect vertical density stratification minima (pycnostads) and maxima (pycnoclines) applied to individual Argo profiles yielded global ocean climatologies of subtropical mode waters and the permanent pycnocline (Feucher et al. 2019). This work greatly refined the canonical schematic for the density and spatial distribution of the mode water (Hanawa & Talley 2001) and provided a new schematic for the permanent pycnocline.

Argo-based climatologies also encouraged novel approaches to distill the mean global ocean thermohaline structure. For example, by applying multivariate functional principal component analysis to a modern climatology (Schmidtko et al. 2013), the thermohaline structures in the top 2 km of the global ocean were decomposed into vertical thermohaline modes, with the first three modes capturing more than 92% of the observed temperature-salinity variance (Pauthenet et al. 2019).

Displacements of Argo floats at their 1000-dbar nominal parking pressure provide velocity data there (e.g., Ollitrault & Rannou 2013), allowing construction of global ocean 1000-dbar velocity climatologies (e.g., Ollitrault & Colin de Verdière 2014). Climatologies of ocean steric height relative to 2000 dbar based on Argo data readily depict major geostrophic flow features including subtropical and subpolar gyre interiors with varying depth penetration (e.g., Roemmich

& Gilson 2009). Combined with the Argo-based mean circulation near 1000-dbar derived from the Argo float displacements, Argo-based steric height climatologies delineate detailed relationships among the upper geostrophic circulation, mode waters, and the permanent pycnocline (Feucher et al. 2019).

The 1000-dbar absolute velocity field is crucial to capture mean geostrophic flow below the permanent pycnocline. Argo data reveal striking sub-thermocline zonal jets of alternating sign with short meridional scales and long zonal coherence in the tropical Pacific; signatures of two apparently distinct systems of altering westward and eastward jets (Cravatte et al. 2017; Figure 2). The1000-dbar Argo velocity field was also used with a full depth temperature and salinity climatology to obtain the full-depth mass transports of the global ocean, revealing interior transports roughly twice those derived from wind stress curl fields, suggesting an important contribution of bottom torque (Verdière & Ollitrault 2016).

2.2 Seasonal Cycles

Seasonal cycles of three-dimensional temperature and salinity fields delineated by the Argo monthly climatology are largely consistent with seasonal climatologies of sea-surface temperature, air-sea fluxes, and sea-surface height (Roemmich & Gilson 2009), as well as wind-driven circulation theory (Giglio et al. 2013). An Argo seasonal mixed layer climatology demonstrates that temperature changes dominate the seasonal cycle of mixed layer density in most regions, but salinity changes are dominant in the tropical warm pools, Arctic, and Antarctic (Johnson et al. 2012).

More than 12 years of Argo data along with more than 22 years of altimetry allow a detailed description of the upper-ocean seasonal march in the equatorial Pacific (Gasparin & Roemmich 2017), including the superposition of a downwelling eastward intraseasonal Kelvin wave on a downwelling westward propagating seasonal Rossby wave. The dominance of an annual Rossby wave in both the isothermal displacement and velocity fields at 1000 dbar was also demonstrated using Argo data (Zanowski et al. 2019).

2.3 The Surface Mixed Layer

The ocean surface mixed layer is a highly temporally and spatially variable feature that contributes to the exchange of heat and freshwater between the atmosphere and the ocean, water mass formation and other numerous physical, chemical, and biological processes. A monthly climatology of mixed-layer depth (MLD) from Argo data was constructed in the previously data-poor Southern Ocean by applying the standard density and temperature threshold method (de Boyer Montegut et al. 2004) to individual Argo profile data (Dong et al. 2008), illuminating mode water formation there. A similar methodology was applied to the global Argo data to provide global monthly mixed layer depth climatology (Hosoda et al. 2010).

A new algorithm was developed to find the MLD of individual Argo profiles (Holte & Talley 2009). A monthly global mixed layer climatology was calculated using both the algorithm and the standard threshold method to demonstrate generally better accuracy of the former (Holte et al. 2017). A mixed layer climatology based on the algorithm has been merged with an

isopycnally based subsurface climatology to provide a consistent three-dimensional climatology on regular pressure grids that better preserves near-surface structure, water-mass properties, and pycnocline strength (Schmidtko et al. 2013).

3. Innovative Insights into Ocean Phenomena from Basin Through Fine Scales

This section reviews the global insights Argo has allowed into key ocean phenomena including subduction of water from the mixed layer to the ocean interior, including fronts, eddies, mixing, and diffusion.

3.1 Subduction

The surface mixed layer lies between the atmosphere and the oceanic pycnoclines below. It directly exchanges properties including heat, freshwater, carbon dioxide, and oxygen with the atmosphere. Subduction is the main mechanism for the transfer of fluid from the mixed layer to the permanent pycnocline. Subduction is driven by Ekman pumping, by lateral induction when horizontal currents flow across a sloping mixed-layer base, and by mesoscale eddies. Understanding how, where, and how much subduction occurs is vital to understanding roles of the ocean in the Earth's climate system and its evolution.

Argo data have been used to further the understanding of subduction processes in all oceanic basins and have revealed new details about their spatio-temporal patterns. For instance, the ventilation of the 18°C Water in the subtropical North Atlantic is driven by vertical pumping near the coast, and the horizontal and temporal structure of the mixed layer depths elsewhere

(Trossman et al. 2009). In the North Pacific subtropical gyre, the westernmost mode waters are not directly subducted in the permanent pycnocline. They are entrained in the mixed layer further to the east the following winter and precondition the subduction of the easternmost mode water (Oka et al. 2011). In the Southern Ocean, subduction is regionally variable with bathymetrically constrained hotspots of large subduction (Sallee et al. 2010).

Argo's four-dimensional observations of temperature and salinity allow investigation of the subduction and propagation of density-compensated temperature-salinity anomalies (spiciness) in the pycnocline (Portela et al. 2020, Sasaki et al. 2010), which may play an important role in decadal climate variability. They also allow accurate estimates of the annual mean subduction rate with much more certainty than those deduced from sporadic hydrographic and tracer data or numerical models (Qu et al. 2016, Toyama et al. 2015).

3.2 Fronts

Oceanic fronts are often boundaries between two different water masses; characterized by large horizontal density gradients; and associated with relatively narrow, deep-reaching current cores and large surface velocities. Those currents play crucial roles in Earth's climate by redistributing oceanic properties, such as heat, freshwater, and nutrients. For example, the Antarctic Circumpolar Current (ACC) is the world's largest current and key to Southern Ocean influence on Earth's climate. It is composed of a set of well-separated fronts. Their properties, positions, and variability have been major research subjects over the Argo era (e.g., Giglio & Johnson 2016). Owing to the Argo's unprecedented sampling, this challenge could be met through the use

of classical methods based on combinations of water mass and dynamic properties (Giglio & Johnson 2016) and more objective methods such as unsupervised classification technique (Jones et al. 2019). With a better knowledge of the fronts' characteristics, it was then possible to investigate their impacts on the Southern Ocean dynamics such as the impact of cross-frontal exchange on the downstream evolution of Sub Antarctic Mode Water properties (Holte et al. 2013) or the link between frontal positions and the sign of eddy-induced subduction (Sallee et al. 2010).

Many studies built on the complement between Argo and other datasets to investigate the impact of fronts on ocean dynamics and biogeochemistry. Together, the Aquarius satellite and Argo data well-resolve detailed features and interannual variations of the sea surface salinity front along the equator (Qu & Yu 2014). In the Mediterranean Sea, biogeochemical (BGC) data from Argo floats and gliders highlighted the relevance of fronts in triggering primary production at the level of the deep chlorophyll maximum (Olita et al. 2017).

3.3 Ocean Footprints of Hurricanes

Tropical cyclones derive their energy from warm upper ocean temperatures. Their strong winds also drive vertical ocean mixing ocean, together leading to cooler sea surface temperatures in the storms' wakes. These cold wakes have been studied using targeted profiling floats in process studies (e.g., Mrvaljevic et al. 2013). Chance encounters between tropical cyclones and Argo floats also provide insight to the basin-wide and global impact of these cold wakes. Argo observations were used to study the interaction between the ocean and Cyclone Nargis (2008) to

understand its rapid intensification (Lin et al. 2009). While the sea surface temperature signature of cold wakes in the North Pacific disappear in about 10 days, Argo shows their subsurface signatures persist for longer than a month (Park et al. 2011). Furthermore, on average, within the radius of gale force winds for strong tropical cyclones, there is a mixed layer heat loss of ~160 MJ m^{-2}. On the global scale, tropical cyclones are estimated, using Argo data, to account for a substantial amount (1.87 PW) of the net annual heat transfer from the ocean to the atmosphere (Cheng et al. 2015).

3.4 Eddies

Oceanic mesoscale eddies with length scales of about 50 to 300 km are ubiquitous, coherent ocean structures. They impact all dynamical components of the oceans and are key contributors to oceanic transports of heat, freshwater, dissolved CO_2, and other water properties, thereby influencing global climate change and the distribution of natural marine resources.

Vertical profiles from Argo floats systematically combined with satellite altimetry observations have afforded three-dimensional eddy reconstructions used to investigate eddies' characteristics and vertical structure at regional (e.g., Chaigneau et al. 2011) and global (Zhang et al. 2013) scales, and their impact on the thermohaline structure of the ocean. Those reconstructions have been subsequently used to estimate the proportion and pathways of the eddy-induced heat transport (Sun et al. 2019, Zhang et al. 2014), confirming that mesoscale eddies trapping and transporting water masses within their core as they propagate can advect large amounts of mass, heat, and freshwater (Dong et al. 2014). Agulhas Rings and their role in advecting large

quantities of heat across the South Atlantic basin are a striking example (Laxenaire et al. 2019; 2020).

The global nature of the Argo array offers unique opportunities to investigate the impacts of eddies on various oceanic processes such as Southern Ocean ventilation (Sallee et al. 2010) and mixed-layer depths at global scale (Gaube et al. 2019), or to produce maps of eddy-derived quantities such as eddy available potential energy (Roullet et al. 2014) and eddy diffusivity at 1000 m (Roach et al. 2018).

3.5 Mixing and Diffusion

The ocean is stirred and mixed by processes across a range of spatial scales. Observational investigations of stirring and horizontal eddy diffusivity in the upper ocean on the global scale would not be possible without Argo data (Cole 2017). The observed geographic distribution of horizontal eddy diffusivity varies by orders of magnitude (Figure 3), with the largest values in the strong current regions (Cole et al. 2015). Argo float trajectory data have been used to estimate Southern Ocean eddy diffusivity using a Lagrangian framework (Roach et al. 2016). This analysis, expanded to the global ocean (Roach et al. 2018), is consistent to within a factor of 2–3 of results from Cole et al. (2015), indicating their robustness. Vertical mixing processes can also be quantified from Argo data: Global maps of turbulence from a parameterization of fine-scale mixing applied to Argo profile observations illuminate the rich spatial and temporal variability of mixing in the ocean (Whalen et al. 2015).

4. Interannual-to-Decadal Variations

Observation of interannual to decadal (I-D) ocean variability is a key Argo objective (Argo Science Team 1998). Ocean and climate phenomena with substantial I-D variability include El Niño/Southern Oscillation (ENSO), meridional overturning circulations (MOCs), gyre circulation changes (Roemmich et al. 2016), marine heat waves (Oliver et al. 2020), and water mass properties and formation rates. As discussed below, Argo data have been sufficient to average over mesoscale variability and extract large spatial scale I-D patterns and their temporal evolution since about 2004 over much of the global ocean.

4.1 ENSO

ENSO is a major, global-scale climate phenomenon, driven by atmosphere-ocean interaction in the tropical Pacific Ocean and involving zonal displacement of very warm water across the tropical Pacific. Changing oceanic conditions there co-vary with vertical convection in the troposphere driven by SST variability, and exert global impacts through atmospheric teleconnections. The evolution of the tropical Pacific permanent thermocline is key to understanding ENSO.

Interannual variations of heat transport and warm water volume associated with ENSO have been quantitatively described using Argo data (Roemmich & Gilson 2011). Similarly, ENSO-related redistributions of heat between surface and subsurface layers have been evaluated globally (e.g., Johnson & Birnbaum 2017). Heat transport and redistribution associated with ENSO cause steric height variations. Argo aids understanding of sea-surface height (SSH)

variability in terms of its steric and mass-related components (Piecuch & Quinn 2016). Interannual surface and subsurface salinity variability related to ENSO is also observed in Argo profiles (Nagano et al. 2017) related to SSH and advection (Gasparin & Roemmich 2016).

4.2 Atlantic Meridional Overturning Circulation (AMOC)

The AMOC consists of a net northward flowing upper layer in the Atlantic, balanced by net southward flow of deeper and denser waters. These opposing transports, of order 15 Sv, vary with latitude and time. The northward meridional heat transport (MHT), closely related to this overturning cell, of order 1 PW, is climatically important. Observations of the AMOC and MHT have been made at several latitudes, using several methodologies (Frajka-Williams et al. 2019).

In the Atlantic at 41°N the flow is weak near the coasts, so broad-scale geostrophic transport from Argo with satellite altimetry gives an accurate representation of the basin-wide total northward limb of the AMOC, estimated as 17.6 Sv with no apparent trend between 2002 and 2009 (Willis 2010). An update of this analysis reveals a decrease from 19 to 17 Sv in the 5-year running mean transport relative to 1000 dbar between 2008 and 2016. The combination of Argo and satellite altimetry was also used in estimates of the AMOC transport in the South Atlantic (Majumder et al. 2016), with results consistent with other methodologies.

Argo data are fundamental for closing the Atlantic heat budget. Air-sea flux estimates combined with Argo oceanic heat storage obtain the oceanic heat transport (Trenberth & Fasullo 2017) by

integrating heat divergence southward from 90°N to any latitude of interest. Results were mostly consistent with MHT estimates using other methods.

4.3 Ocean Circulation Changes

Variability of large-scale wind forcing of the ocean causes spin-up or down of the oceanic circulation, affecting mass, heat, and freshwater transport. Argo temperature and salinity profiles are used to calculate relative geostrophic current in the upper layer of the global ocean. In addition, trajectory data obtained from float positions directly document current velocity at the drifting pressure of Argo floats, enabling estimation of absolute ocean velocity profiles.

Using Argo data, climatological meridional transports are estimated in each ocean basin for interior circulations and boundary currents. For example, net northward transport in the South Pacific Ocean is estimated as 20.6 ±6.0 Sv across 32°S (Zilberman et al. 2014), with interannual variability proportional to the Southern Annular Mode. For all ocean basins evaluation of the Sverdrup balance (Gray & Riser 2014) demonstrates consistency of wind stress and meridional geostrophic transport from Argo, especially in the tropics and subtropics.

The large volume of Argo data allows ocean velocities to be decomposed into average and eddy components (Katsumata 2016). Using surface topographic data from satellites, along with Argo and WOCE hydrography, long-term changes associated with acceleration of upper-ocean circulation are estimated (Giglio et al. 2012, Roemmich et al. 2016). With further accumulation

of Argo profiles and trajectory data, gyre circulation variability and related heat and freshwater transport are described quantitatively.

4.4 Marine Heat Waves

Globally, long-term ocean warming is strongest at the surface, diminishing with depth (e.g., Wijffels et al. 2016). Therefore, the mean stratification of the surface layer is increasing as SST increases. Regional variability of SST warming results in strong seasonal to interannual warm anomalies termed marine heat waves (MHWs; Oliver et al. 2021). Large persistent MHWs occurred in 2009–2010 in the central South Pacific, 2013–2016 and 2019–2020 (Scannell et al. 2020) in the northeast Pacific (Figure 4), and 2015–2019 in the Tasman Sea (Chiswell & Sutton 2020).

Strong and persistent MHWs have profound impacts on marine ecosystems that may lead to economic losses and other societal impacts. MHWs drive migratory responses, and may cause decreased primary production, large-scale coral bleaching, toxic algal blooms, and declines in commercial fisheries. The addition of biogeochemical sensors to Argo floats, BGC Argo, will enable more comprehensive knowledge of ecosystem responses to MHWs. With Argo's global coverage, the relationship between increased stratification and decreased primary productivity can be more widely tested (e.g., Chiswell & Sutton 2020, Lozier et al. 2011).

Argo advances understanding of MHWs by revealing their subsurface structure and evolution (Figure 4). The Argo dataset enables estimates of mixed-layer heat storage and advection terms

that are important contributors, along with air-sea heat flux and mixing/entrainment, to formation and duration of MHWs. MHW causality is complex, but anomalously weak air-sea heat loss and oceanic advection were factors in the 2013–2016 NE Pacific episode (Bond et al. 2015) and salinity variability played a role in the 2019–2020 MHW there (Scannell et al. 2020). Argo's global coverage and expanding longevity will enhance the ability of ocean-atmosphere modeling to close the mixed layer heat budget and predict MHW evolution.

4.5 Water-Mass & Subduction Variability

Water masses, defined by their temperature-salinity characteristics, are formed by wind and buoyancy forcing at the sea surface. As newly formed waters are separated from the sea surface, specific water masses are identified as mode waters, intermediate waters, deep waters, and bottom waters depending on their depth. Argo float data enable accurate documentation of water masses, including mode waters globally (Feucher et al. 2019), and investigation of contributions of mode water to the interannual variability of ocean heat content (Kolodziejczyk et al. 2019). The uniform and global Argo data set allows observation of interannual variability of water masses in greater detail than previously possible (Oka et al. 2015, Piron et al. 2017), and in locations where ship observations are challenging, such as the Southern Ocean (Giglio & Johnson 2016).

Water mass property and volume anomalies contain the ocean's memory of climate fluctuations, subducted subsurface and advected by ocean circulation. The processes, variability, and rate of subduction are estimated in detail from Argo data (Qu et al. 2008, Toyama et al. 2015). A

weakening subduction rate associated with global warming is estimated as -3.44±2.47 m yr^{-2} (Wang et al. 2015). Variation in obduction (subduction's opposite) are also important for reemergence of climate signals (Kawai et al. 2021).

5. Global Climate Insights and Synergies with Satellites

Argo data, together with historical ocean and satellite data, provide valuable insights into long-term ocean trends central to understanding climate change and projecting future climates, including ocean warming, sea level rise, ocean salinity changes reflecting hydrological cycle changes, and increases in ocean stratification.

5.1 Earth's Energy Imbalance

Owing to the build-up of atmospheric greenhouse gasses and the massive thermal inertia of the ocean, order 1 W m^{-2} more energy enters the top of the atmosphere (TOA) than exits it (Hartmann et al. 2014). This difference is often referred to as Earth's Energy Imbalance (EEI). Accurately measuring the small (<0.3%) difference of large spatially and temporally variable numbers at the TOA is very difficult. Thus, most estimates of EEI have focused on changes of heat energy storage in the climate system (von Schuckmann et al. 2020). For the ocean, which has absorbed about nine tenths of the EEI over the past few decades, this means estimating global integrals of temperature changes.

Pioneering ocean warming estimates prior to Argo (Levitus et al. 2005) suffered from effects of sparse spatial coverage and systematic instrumental measurement biases (Domingues et al.

2008). Since 2005, over 15 years of high-quality, year-round, near-global Argo ocean temperature data greatly advanced estimates of ocean warming rates. First, reliable seasonal cycles of temperature and salinity can be estimated locally throughout the globe using Argo (Roemmich & Gilson 2009), vital for assessing anomalies in these variables from data taken in any time of year either during the Argo era, or as early as the Challenger Expedition of the 1870s (Roemmich et al. 2012). Second, Argo data's high quality has prompted investigations into instrumental biases (most notably those arising from variations in fall rates and temperature calibrations of expendable bathythermographs, or XBTs, which comprise a substantial fraction of the global ocean temperature database from 1967 through the mid-2000s (Abraham et al. 2013, Cheng et al. 2014, Gouretski & Reseghetti 2010). Third, sampling in Argo years is so increased that it, coupled with the high quality of the data, greatly reduce the uncertainty of the EEI (mostly ocean warming) from 0.6 (±0.4 W) m^{-2} from 2005–2010 to about 0.7 (±0.1) W m^{-2} from 2005–2015 (e.g., Johnson et al. 2016, Wijffels et al. 2016).

The warming trend detected by Argo is largest at the surface in the global average, but can be seen all the way to the core array's 2000-dbar profiling pressure (Johnson et al 2019a). Regional pilot arrays of Deep Argo floats profiling to full depth are detecting warming trends below 2000 dbar (Johnson et al. 2019b; 2020), most prominently in the bottom waters spreading north from Antarctica, quantified previously by ship-based repeat measurements (Purkey & Johnson 2013), that amount to about one tenth of the total EEI (Johnson et al. 2016, von Schuckmann et al. 2020). In addition, regional patterns of warming can be estimated using Argo and other data, and related to climate variations (Johnson & Lyman 2020).

5.2 Sea Level Rise

Ocean warming contributes directly to sea level rise through thermal expansion of seawater, accounting for about 40% of the globally integrated trend from 1993 through ~2016 (Cazenave et al. 2018). The other 60% comes from transfers of water (mostly melting ice) from the land to the ocean. While freshening from this melt also causes sea level rise by reducing seawater density, that contribution is much smaller than the other two terms in the global average (Munk 2003). Strong synergies among Argo and data from two different sets of instruments on satellites allow quantification of the contributions. Satellite altimeters (from Jason[1] and other missions), measure anomalies in sea level to great precision at all but the highest latitudes. Satellite gravimeters (GRACE and its follow-on) measure temporal variations in the gravity field of Earth, from which ocean mass changes are estimated. Knowing the variations in sea level owing to thermal expansion from Argo, the changes in ocean mass from GRACE, and the changes in sea level from Jason and other altimeter missions allows balancing of the sea level budget (Leuliette 2015), with excellent agreement down to monthly time scales (Figure 5).

5.3 Salinity and the Hydrological Cycle

About 86% of evaporation and 78% of precipitation occurs over the ocean, with most of the balance returning to the ocean as run-off from the land (Schanze et al. 2010). As the atmosphere warms it can hold more water, which means more evaporation in some regions, and more

[1] The name Argo invokes the synergies between the Jason satellite altimeter missions and the Argo Program by recalling the legend of Jason and the Argonauts, who sailed the ship *Argo* in search of the Golden Fleece.

precipitation in others. Precipitation is extremely patchy and difficult to measure, especially over the ocean, where rain gauges can only be located on islands and buoys. (Although passive acoustic listening devices have been deployed on a few floats to measure rainfall (Yang et al. 2015), and more recently satellite measurements (Hou et al. 2014) provide global, but not continuous, estimates.) However, changes of ocean salinity can approximate a combination evaporation pan and rain gauge (Durack 2015). The net removal of freshwater by evaporation (or ice formation) and build-up from precipitation (or river run-off and ice melt) in the upper ocean over large spatial scales are reflected in salinity changes (absent changes in ocean mixing or advection). Again, Argo, by allowing determination of a seasonal cycle in salinity around much of the globe, has improved the ability to analyze historical data and determine trends in upper ocean salinity over decades.

Changes in surface salinity between historical (1960–1989) and Argo (2003–2007) data are consistent with an increase in evaporation in salty (e.g., subtropical) regions and an increase in precipitation in fresher (e.g., subpolar and tropical) ocean regions, as expected with a warming atmosphere (Hosoda et al. 2009). Increases from 1970 to 2005 in net values of precipitation minus evaporation over the ocean have been estimated from subsurface salinity changes at between -3% and +16% depending on region. (Helm et al. 2010). Both subsurface and surface salinity trends estimated from 1950 to 2008 are also consistent with an increase in the hydrological cycle, including on basin scales, with the Atlantic becoming saltier and the Pacific fresher, and more local scales, with the Bay of Bengal freshening as the Arabian Sea becomes saltier (Durack & Wijffels 2010).

5.4 Stratification Changes

Ocean warming and amplification of existing salinity patterns have generally been surface-intensified. This pattern has led to an increase in stratification of several percent since 1960, with the bulk of that change owing to warming in the upper ocean, augmented at high latitudes and in the tropics by freshening and slightly offset in the subtropics by salinity increases (Li et al. 2020). Stratification increases have strong implications for climate, biogeochemistry, and ecosystems.

6. Argo Data Improve Ocean, Weather, and Climate Models

Argo data are routinely assimilated into ocean forecast, reanalysis, and seasonal prediction systems, and are used to ground-truth multi-year predictions and climate projections. Argo data are also increasingly used to initialize coupled numerical weather prediction (NWP) systems. Without Argo data, the quality of most ocean forecasts and reanalyses, and most seasonal predictions, would be of substantially lower value.

6.1 Ocean Forecasting and Reanalysis Systems

Ocean forecasting now underpins the operation of many marine industries (Bell et al. 2015). All credible ocean forecast systems (OFSs) assimilate Argo data, together with satellite data, to initialize the ocean state (e.g., Cummings et al. 2009). Initialized ocean models are integrated forward in time – typically for 7 days – forced by surface fluxes from an NWP system. Ocean forecasts are widely used for safety at sea, efficiency, and conservation.

Many Ocean Reanalysis Systems, or ORAs (Storto et al. 2019), have been developed in parallel with OFSs. They often use the same underlying model, and the same data assimilation system. Some ORAs are eddy-resolving (e.g., Artana et al. 2019), some are eddy-permitting (e.g., Carton & Giese 2008), and some are coarse resolution (e.g., Balmaseda et al. 2013). All ORAs assimilate Argo data, and depend on Argo data to constrain subsurface ocean properties (Storto et al. 2019).

Most OFSs/ORAs have been used to quantify the impact of Argo (and other) data on their forecasts/reanalyses (e.g., Fujii et al. 2019, Oke et al. 2009). After withholding Argo data from the UKMet's operational OFS for only one month, the global-averaged forecast errors for upper-ocean temperature and salinity increased by more than 5%, with increased errors exceeding 2 degrees at 100 m depth for many parts of the ocean (Lea et al. 2015). Withholding Argo data from the latest version of ORAS4 (Zuo et al. 2019), a coarse-resolution ocean reanalysis shows that without Argo data, these types of reanalyses become unsuitable for realistically representing ocean variability (Fujii et al. 2019, Figure 6). These results are typical for many OFSs/ORAs.

Most OFSs/ORAs have long been plagued by deep biases in temperature in salinity, largely a consequence of scant deep measurements. A 1200-float Deep Argo array (Johnson et al. 2015) promises to solve this problem. Constructing a synthetic database of Deep Argo measurements from one model and assimilating those synthetic observations into a different model showed that

assimilation of data from Deep Argo floats may reduce the errors of temperature and salinity in the deep ocean (below 2000 m depth) by as much as 50% (Gasparin et al. 2020).

6.2 Seasonal Prediction

Seasonal prediction systems (SPSs) typically employ coupled ocean-atmosphere models, and increasingly, coupled earth-systems models (including sea-ice and land-surface models). SPSs usually forecast with lead times of 3 months to 1 year. Most of the skill of SPSs stems from the ocean initialization and results from the longer timescales of variability (the "memory") of the ocean (Balmaseda & Anderson 2009, Huang et al. 2021). Argo data are therefore the most critical ocean observations for initializing seasonal forecasts.

Many studies have assessed the impact of Argo data on seasonal prediction skill. Some studies have compared the skill of seasonal predictions for pre-Argo periods versus contemporary periods when the Argo is near-global with mixed results (Huang et al. 2021, Kumar et al. 2015). Interpretation of results from these studies is problematic owing to differences in the predictability of the climate for these periods. For example, many relevant metrics were more predictable before 2000 (the pre-Argo period) than afterwards (Zhao et al. 2016). Withholding Argo data and performing seasonal predictions for the same periods and events arguably provides better assessments, and all such studies find positive impacts. For example, assimilation of Argo data reduces forecast errors of temperature at 3-months lead time by 0.2 degrees in the western equatorial Pacific, and increases the correlation skill of ENSO-related metrics by 0.1–0.2 at 4-months lead time (Balmaseda et al. 2013). Inclusion of Argo data extends the forecast time

for meaningful ENSO forecasts by 1.5 months (Stockdale et al. 2018). Many other similar studies also make clear that seasonal predictions benefit from Argo data, with increased skill at increased lead time.

6.3 Coupled Numerical Weather Prediction (NWP)

Most NWP centers are moving towards coupled atmosphere-ocean models for short-range (~7-day lead time) weather forecasting. As coupled systems are adopted, Argo data's importance and impact for NWP will certainly increase. However, despite the long-understood potential benefits of coupled prediction (Emanuel 1999), progress has been slow owing to significant scientific and technical challenges. Consequently, there are so far very few studies (King et al. 2020) that have explicitly assessed the impact of Argo data on coupled NWP.

In general, coupled NWP prediction has shown greater positive impacts, compared to traditional atmosphere-only, for longer lead-time forecasts. For example, forecasts of the Madden-Julian Oscillation have greater skill from a coupled system, compared to an uncoupled system, for lead times of greater than 10 days (Woolnough et al. 2007). Coupled systems outperform atmosphere-only systems more at lower latitudes (Vellinga et al. 2020), with more neutral benefit of coupled NWP at mid-latitudes reported (Lea et al. 2015). Here, improved forecast skill can largely be ascribed to the ocean initialization using Argo data. For extreme events (e.g., Hurricane Sandy, in October 2012 in the North Atlantic), coupled prediction yields a better forecast of the timing and location of the hurricane's landfall than traditional NWP (King et al. 2020). This

improvement is ascribed to the better representation of the Gulf Stream position in the coupled system, largely attributed to the impact of Argo data.

Widespread adoption of coupled NWP is progressing. The greatest challenge is consistent initialization of the atmosphere and ocean components of the coupled system, largely being tackled by coupled data assimilation (distinct from uncoupled assimilation). Coupled data assimilation is challenging, allowing oceanic observations—including Argo data—to directly influence analyses of the atmosphere and vice versa, but progressing (e.g., Fujii et al. 2021). The next generation of NWP systems will likely all rely on coupled ocean-atmosphere systems. For those systems, Argo data will be a foundational source of data for coupled initialization.

6.4 Decadal Prediction and Climate Projection

Much like coupled NWP, decadal prediction, increasingly referred to as near-term climate prediction (Kushnir et al. 2019), has been hampered by difficulties achieving consistent initialization of ocean and atmospheric models. Researchers have explored, with mixed results, coupled data assimilation (Fujii et al. 2021), parameter estimation (Zhang et al. 2020), multi-model ensemble prediction (Meehl et al. 2014), and other more basic (Brune & Baehr 2020) – but perhaps still useful – approaches to initialization. Argo was quickly recognized as the most critical observation platform for initializing decadal predictions (Meehl et al. 2009). A modeling study, without data assimilation, demonstrated that decadal prediction of ocean heat content should be skillful (Yeager et al. 2012). Initializing the ocean with an Argo-based gridded product gave promising results (Robson et al. 2012), but model drift and coupled initialization remain as

challenges. Ongoing efforts routinely rely upon Argo data for initializations (Kushnir et al. 2019).

Climate projections do not assimilate observations (Eyring et al. 2016). But climate mode outputs are routinely compared to Argo (and other) data to assess their representation of contemporary periods (e.g., Voldoire et al. 2019). This includes comparisons of mixed-layer depths (e.g., Roberts et al. 2020), upper-ocean heat content (e.g., Buckley et al. 2019), mean upper-ocean temperature and salinity (e.g., Robson et al. 2020), and even Argo-derived diffusivity (Zhu et al. 2020). Argo data clearly play an important role in the validation of systems used for climate projections, providing a comprehensive ground-truth that guides model development and model tuning.

Summary Points

- The Argo Array, which started with a few floats in 2000, now observes temperature and salinity in the upper half of the ocean volume (to 2000 m) for its core mission, with almost 4000 active floats distributed over most of the global ocean.
- Now numbering over 2 million, high-quality profiles from core Argo, reported in near real-time, have underpinned over 4000 scientific papers, and are routinely used to improve ocean, weather, and climate forecasts and nowcasts.
- Ocean climatologies (of the long-term mean, seasonal cycle, or monthly values) using temperature, salinity, and velocity data have confirmed existing theories, allowed novel discoveries, and prompted new hypotheses regarding ocean circulation, water mass formation, and their drivers.
- Analyses of Argo data have also illuminated diverse oceanic physical processes, including water-mass formation, subduction, eddy influences on ocean circulation and water masses, frontal structure and dynamics, and even global patterns of mixing and diffusivity.
- The Argo record, now approaching two decades in length, is increasingly allowing insightful analyses of interannual to decadal ocean variability, including the global redistributions of heat and salt with ENSO, variations in gyre and meridional overturning circulation strength, and the evolution of marine heat waves, to name a few.
- Argo data, combined with historical in situ observations and contemporaneous satellite data, have illuminate key climate phenomena with greatly increased certainty, including Earth's Energy Imbalance, contributions of ocean warming versus land ice melting to sea

level rise, and increases in the hydrological cycle with atmospheric warming as observed by amplification of ocean salinity patterns.

- Argo data have been key to advances in ocean reanalyses that combine various observations in a dynamical framework to fill gaps in observations, ocean and weather nowcast and forecasts, as well as validating the ability of climate models to represent contemporary ocean conditions.

Future Issues

- Core Argo, the mission measuring physical parameters from 0-2000 m, will extend its capabilities through expansion into marginal seas and seasonally ice-covered regions in the climate critical, rapidly warming high latitudes, as well as increases in float numbers in the dynamic tropics and western boundary current extensions.
- Deep Argo has begun regional pilot arrays, with the goal of over 1200 floats reporting measurements from the sea surface to the sea floor to monitor deep ocean warming and circulation changes.
- BioGeoChemical (BGC) Argo, which aims to add oxygen, nitrate, pH, fluorescence, optical backscatter, and downwelling irradiance sensors to 1000 floats deployed around the globe, will greatly expand the contributions of Argo beyond the physical realm.
- Synergies with new observing system elements will increase the usefulness of Argo data, including the new surface water and ocean topography altimeter for sub-mesoscale oceanography, and glider arrays for coastal and boundary current interactions with the open ocean.

- Argo data will become increasingly vital for climate and weather forecasts as progress is made in the challenging task of initializing coupled models.
- Continued improvements in sensor accuracy and stability, as well as float and sensor energy efficiency and longevity, will be crucial in maintaining and improving the Argo array.

Acknowledgements

PMEL contribution number 5210. GCJ is supported by NOAA Research. Argo data were collected and made freely available by the International Argo Project and the national programmes that contribute to it. Argo is a pilot programme of the Global Ocean Observing System.

Figures

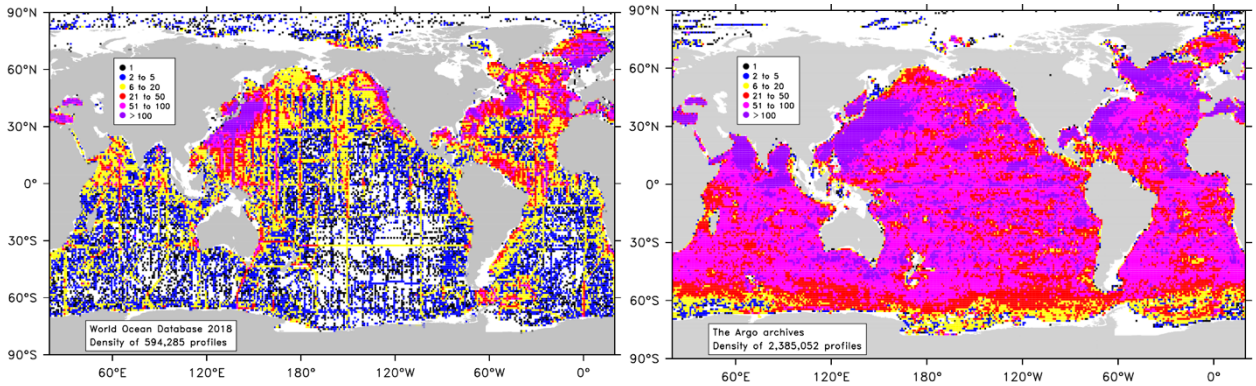

Figure 1. Spatial sampling density (see legend) of subsurface ocean profiles of both temperature and salinity to a depth of 1,000 m or deeper in 1° latitude × 1° longitude bins reported from a) previous historical, largely shipboard expeditions, collected over the past 100 years downloaded from the World Ocean Data Base in January 2018 and b) Argo through mid-February 2021. Updated following Riser et al (2016).

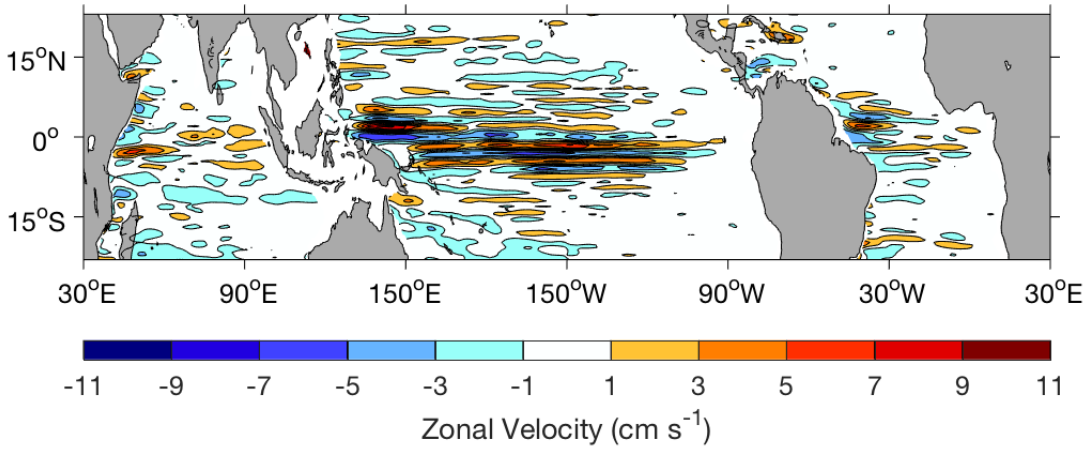

Figure 2. Mean zonal velocity at 1000 dbar pressure estimated from 1000-dbar Argo parking pressure displacements after Zanowski et al. (2019) but expanded from the Pacific to the global tropics.

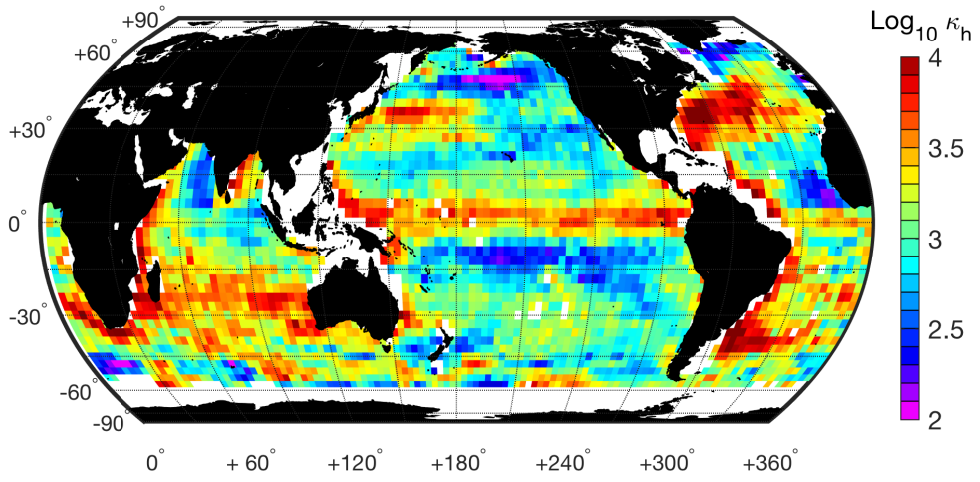

Figure 3:Horizontal eddy diffusivity derived from Argo float temperature and salinity profiles and ECCO-2 eddy kinetic energy at 500 meters depth (in units of m2 s-1, note logarithmic color scale). Courtesy of Sylvia Cole (after Cole et al. 2015, Cole 2017).

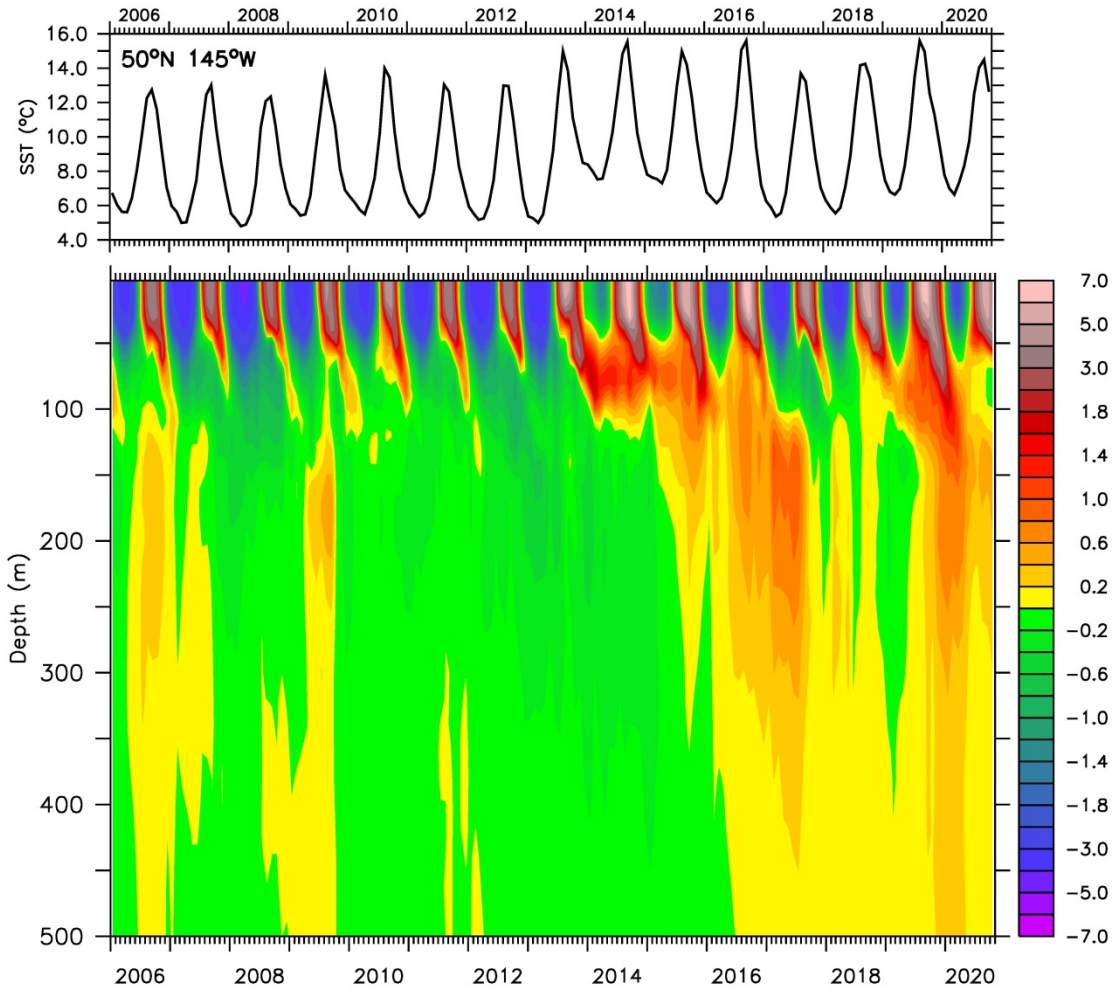

Figure 4. The NE Pacific Marine Heat Wave, here at 50°N 145°W, from Argo data. (Upper) SST. (Lower) Temperature deviation from the 2006 – 2020 mean. The strong summer SST warming in 2013–2016 and 2019–2020 is mixed and/or subducted into subsurface layers.

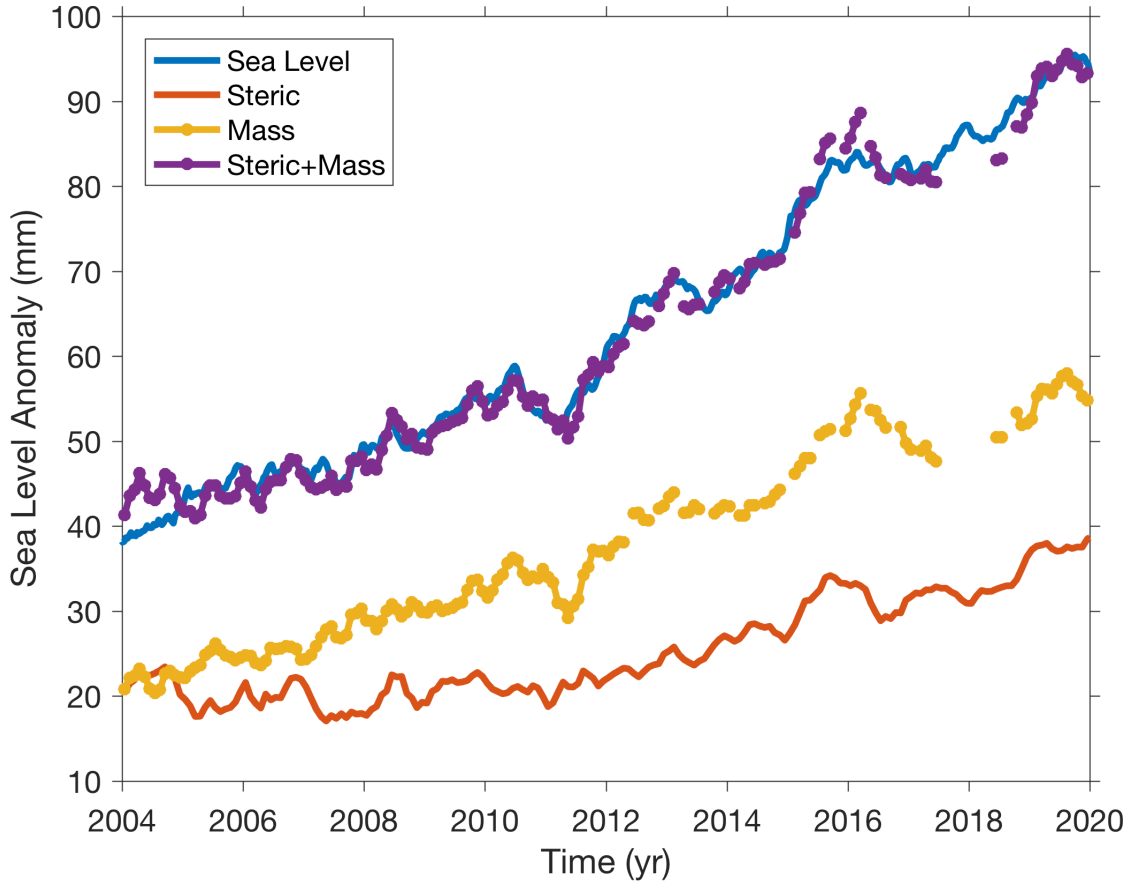

Figure 5. Monthly averaged global mean sea level anomaly (blue line) observed by satellite altimeters from the NOAA Laboratory for Satellite Altimetry. Monthly averaged global ocean mass (yellow line with dots) from the Gravity Recovery and Climate Experiment. Monthly averaged global mean steric sea level (orange line) from the Argo profiling float array. Mass plus steric (purple line with dots). All time-series have been smoothed with a 3-month filter. Modified from Thompson et al. (2020).

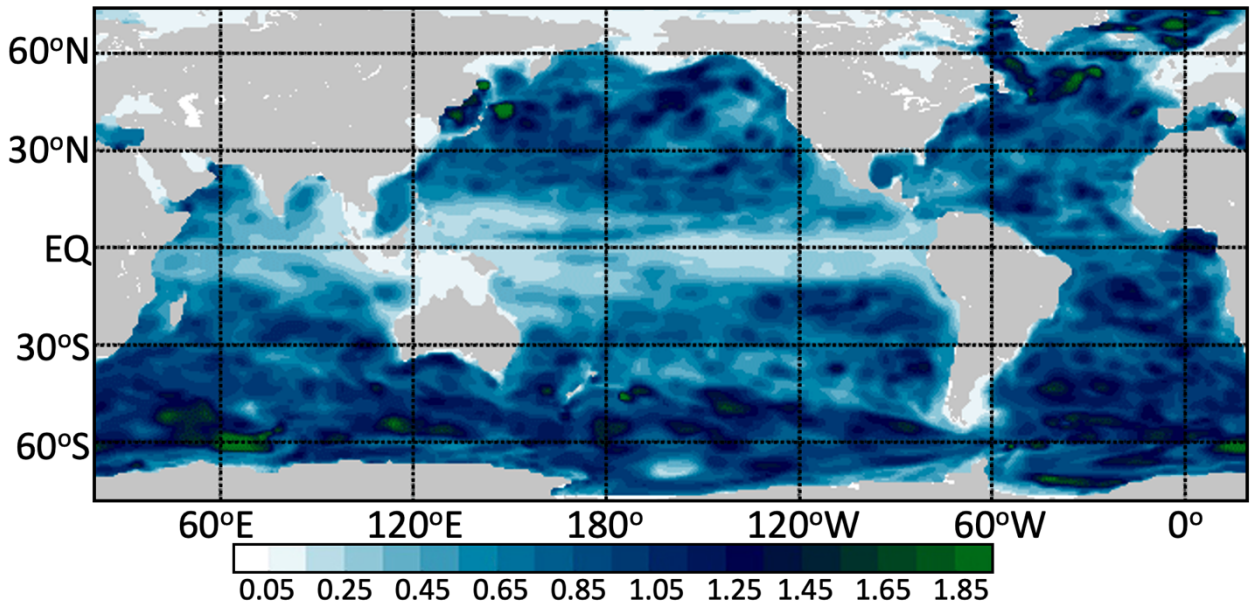

Figure 6: Normalized RMS difference of temperature for the upper 700 m from 2008–2014 between ocean reanalysis ORAS4 with Argo withheld, and with Argo assimilated. Fields are normalized against temporal standard deviations of temperature. Values exceeding unity indicate that errors in the reanalysis due to the neglect of Argo data are comparable to or exceed the signal amplitude. Adapted from Fujii et al. (2019).

Literature Cited

Abraham JP, Baringer M, Bindoff NL, Boyer T, Cheng LJ, et al. 2013. A review of global ocean temperature observations: Implications for ocean heat content estimates and climate change. *Rev. Geophys.* 51:450-83

Argo Science Team. 1998. *On the design and implementation of Argo: an initial plan for a global array of profiling floats*. ICPO Report No. 21 (GODAE International Project Office, Bureau of Meteorology)

Artana C, Provost C, Lellouche J-M, Rio M-H, Ferrari R, Sennéchael N. 2019. The Malvinas Current at the confluence with the Brazil Current: Inferences from 25 years of mercator ocean reanalysis. *J. Geophys. Res. Oceans* 124:7178-200

Balmaseda M, Anderson D. 2009. Impact of initialization strategies and observations on seasonal forecast skill. *Geophys. Res. Lett.* 36:L01701

Balmaseda M, Mogensen K, Weaver AT. 2013. Evaluation of the ECMWF ocean reanalysis system ORAS4. *Q. J. R. Meteorol. Soc.* 139:1132-61

Bell MJ, Schiller A, Le Traon P-Y, Smith NR, Dombrowsky E,Wilmer-Becker K. 2015. An introduction to GODAE OceanView. *J. Oper. Oceanogr.* 8(s1), s2-s11 https://doi.org/10.1080/1755876X.2015.1022041

Bond NA, Cronin MF, Freeland H, Mantua N. 2015. Causes and impacts of the 2014 warm anomaly in the NE Pacific. *Geophys. Res. Lett.* 42:3414-20

Brune S, Baehr J. 2020. Preserving the coupled atmosphere-ocean feedback in initializations of decadal climate predictions. *WIREs Clim. Change* 11:e637

Buckley MW, DelSole T, Lozier MS, Li L. 2019. Predictability of North Atlantic sea surface temperature and upper-ocean heat content. *J. Clim.* 32:3005-23

Carton JA, Giese BS. 2008. A reanalysis of ocean climate using Simple Ocean Data Assimilation (SODA). *Mon. Weather Rev.* 136:2999-3017

Cazenave A, Meyssignac B, Ablain M, Balmaseda M, Bamber J, et al. 2018. Global sea-level budget 1993-present. *Earth Syst. Sci. Data* 10:1551-90

Chaigneau A, Le Texier M, Eldin G, Grados C, Pizarro O. 2011. Vertical structure of mesoscale eddies in the eastern South Pacific Ocean: A composite analysis from altimetry and Argo profiling floats. *J. Geophys. Res. Oceans* 116:C11025

Cheng L, Zhu J, Cowley R, Boyer T, Wijffels S. 2014. Time, probe type, and temperature variable bias corrections to historical expendable bathythermograph observations. *J. Atmos. Ocean. Technol.* 31:1793-825

Cheng L, Zhu J, Sriver RL. 2015. Global representation of tropical cyclone-induced short-term ocean thermal changes using Argo data. *Ocean Sci.* 11:719-41

Chiswell SM, Sutton PJH. 2020. Relationships between long-term ocean warming, marine heat waves and primary production in the New Zealand region. *N. Z. J. Mar. Freshw. Res.* 54:614-635

Cole ST. 2017. Investigating small-scale processes from an abundance of autonomous observations. In *Autonomous and Lagrangian Platforms and Sensors(ALPS II): A Report of the ALPS II Workshop*, pp. 25-27.

Cole ST, Wortham C, Kunze E, Owens WB. 2015. Eddy stirring and horizontal diffusivity from Argo float observations: Geographic and depth variability. *Geophys. Res. Lett.* 42:3989-97

Colin de Verdière A, Ollitrault M. 2016. A direct determination of the world ocean barotropic circulation. *J. Phys. Oceanogr.* 46:255-73

Cravatte S, Kestenare E, Marin F, Dutrieux P, Firing E. 2017. Subthermocline and intermediate zonal currents in the tropical Pacific Ocean: Paths and vertical structure. *J. Phys. Oceanogr.* 47:2305-24

Cummings J, Bertino L, Brasseur P, Fukumori I, Kamachi M, et al. 2009. Ocean data assimilation systems for GODAE. *Oceanography* 22(3):96–109

Davis RE. 2005. Intermediate-depth circulation of the Indian and South Pacific Oceans measured by autonomous floats. *J. Phys. Oceanogr.* 35:683-707

Davis RE, Webb DC, Regier LA, Dufour J. 1992. The Autonomous Lagrangian Circulation Explorer (ALACE). *J. Atmos. Ocean. Technol.* 9:264-85

de Boyer Montegut C, Madec G, Fischer AS, Lazar A, Iudicone D. 2004. Mixed layer depth over the global ocean: An examination of profile data and a profile-based climatology. *J. Geophys. Res.* 109:C12003

Domingues CM, Church JA, White NJ, Gleckler PJ, Wijffels SE, et al. 2008. Improved estimates of upper-ocean warming and multi-decadal sea-level rise. *Nature* 453:1090-3

Dong C, McWilliams JC, Liu Y, Chen D. 2014. Global heat and salt transports by eddy movement. *Nat. Commun.* 5:3294

Dong S, Sprintall J, Gille ST, Talley L. 2008. Southern Ocean mixed-layer depth from Argo float profiles. *J. Geophys. Res. Oceans* 113:C06013

Durack PJ. 2015. Ocean salinity and the global water cycle. *Oceanography* 28:20-31

Durack PJ, Wijffels SE. 2010. Fifty-year trends in global ocean salinities and their relationship to broad-scale warming. *J. Clim.* 23:4342-62

Emanuel KA. 1999. Thermodynamic control of hurricane intensity. *Nature* 401:665-9

Eyring V, Bony S, Meehl GA, Senior CA, Stevens B, et al. 2016. Overview of the Coupled Model Intercomparison Project Phase 6 (CMIP6) experimental design and organization. *Geosci. Model Dev.* 9:1937-58

Feucher C, Maze G, Mercier H. 2019. Subtropical mode water and permanent pycnocline properties in the World Ocean. *J. Geophys. Res. Oceans* 124:1139-54

Folger, T. 1787. Chart of the Gulf Stream. In: *Benjamin Franklin, Philosophical and Miscellaneous Papers*, London: C. Dilly

Frajka-Williams E, Ansorge IJ, Baehr J, Bryden HL, Chidichimo MP, et al. 2019. Atlantic Meridional Overturning Circulation: Observed transport and variability. *Front. Mar. Sci.* 6:260

Fujii Y, Ishibashi T, Yasuda T, Takaya Y, Kobayashi C, Ishikawa I. 2021. Improvements in tropical precipitation and sea surface air temperature fields in a coupled atmosphere–ocean data assimilation system. *Q. J. R. Meteorol. Soc*. https://doi.org/10.1002/qj.3973

Fujii Y, Rémy E, Zuo H, Oke P, Halliwell G, et al. 2019. Observing system evaluation based on ocean data assimilation and prediction systems: On-going challenges and a future vision for designing and supporting ocean observational networks. *Front. Mar. Sci.* 6:417

Gaillard F, Reynaud T, Thierry V, Kolodziejczyk N, von Schuckmann K. 2016. In situ–based reanalysis of the global ocean temperature and salinity with ISAS: Variability of the heat content and steric height. *J. Clim.* 29:1305-23

Gasparin F, Hamon M, Rémy E, Traon P-YL. 2020. How Deep Argo will improve the deep ocean in an ocean reanalysis. *J. Clim.* 33:77-94

Gasparin F, Roemmich D. 2016. The strong freshwater anomaly during the onset of the 2015/2016 El Niño. *Geophys. Res. Lett.* 43:6452-60

Gasparin F, Roemmich D. 2017. The seasonal march of the equatorial Pacific upper-ocean and its El Niño variability. *Prog. Oceanogr.* 156:1-16

Gaube P, J. McGillicuddy Jr. D, Moulin AJ. 2019. Mesoscale eddies modulate mixed layer depth globally. *Geophys. Res. Lett.* 46:1505-12

Giglio D, Johnson GC. 2016. Subantarctic and polar fronts of the Antarctic Circumpolar Current and Southern Ocean heat and freshwater content variability: A view from Argo[*,+]. *J. Phys. Oceanogr.* 46:749-68

Giglio D, Roemmich D, Cornuelle B. 2013. Understanding the annual cycle in global steric height. *Geophys. Res. Lett.* 40:4349-54

Giglio D, Roemmich D, Gille ST. 2012. Wind-driven variability of the subtropical North Pacific Ocean. *J. Phys. Oceanogr.* 42:2089-100

Gillis, J. 2014. In the Ocean, Clues to Change. *New York Times*, August 12, 2014, New York, NY

Gouretski V. 2019. A new global ocean hydrographic climatology. *Atmos. Ocean. Sci. Lett*. 12:226-9

Gouretski V, Reseghetti F. 2010. On depth and temperature biases in bathythermograph data: Development of a new correction scheme based on analysis of a global ocean database. *Deep-Sea Res. Part I-Oceanogr. Res. Pap.* 57:812-33

Gray AR, Riser SC. 2014. A global analysis of Sverdrup balance using absolute geostrophic velocities from Argo. *J. Phys. Oceanogr.* 44:1213-29

Hanawa K, and Talley LD, 2001. Mode Waters. In *Ocean Circulation and Climate*, ed. G Siedler, J Church, J Gould, pp. 373-86. International Geophysics Series, Academic Press.

Hartmann DL, Klein Tank AMG, Rusticucci M, Alexander LV, Brönnimann S, et al. 2014. Observations: Atmosphere and Surface. *Climate Change 2013: the Physical Science Basis. Contribution of Working Group I to the Fifth Assessment Report of the Intergovernmental Panel on Climate Change,* ed. TF Stocker, D Qin, G-K Plattner, M Tignor, SK Allen, et al., pp. 159-254. Cambridge, UK: Cambridge University Press

Helm KP, Bindoff NL, Church JA. 2010. Changes in the global hydrological-cycle inferred from ocean salinity. *Geophys. Res. Lett.* 37:L18701

Holte J, Talley L. 2009. A new algorithm for finding mixed layer depths with applications to Argo data and subantarctic mode water formation. *J. Atmos. Ocean. Technol.* 26:1920-39

Holte J, Talley LD, Gilson J, Roemmich D. 2017. An Argo mixed layer climatology and database. *Geophys. Res. Lett.* 44:5618-26

Holte JW, Talley LD, Chereskin TK, Sloyan BM. 2013. Subantarctic mode water in the southeast Pacific: Effect of exchange across the Subantarctic Front. *J. Geophys. Res. Oceans* 118:2052-66

Hosoda S, Ohira T, Sato K, Suga T. 2010. Improved description of global mixed-layer depth using Argo profiling floats. *J. Oceanogr.* 66:773-87

Hosoda S, Suga T, Shikama N, Mizuno K. 2009. Global surface layer salinity change detected by Argo and its implication for hydrological cycle intensification. *J. Oceanogr.* 65:579-86

Hou AY, Kakar RK, Neeck S, Azarbarzin AA, Kummerow CD, et al. 2014. The Global Precipitation Measurement Mission. *Bull. Am. Meteorol. Soc.* 95:701-+

Huang B, Shin C-S, Kumar A, L'Heureux M, Balmaseda MA. 2021. The relative roles of decadal climate variations and changes in the ocean observing system on seasonal prediction skill of tropical Pacific SST. *Clim. Dyn*. https://doi.org/10.1007/s00382-021-05630-1

Johnson GC, Birnbaum AN. 2017. As El Nino builds, Pacific Warm Pool expands, ocean gains more heat. *Geophys. Res. Lett.* 44:438-45

Johnson GC, Cadot C, Lyman JM, MeTaggart KE, Steffen EL. 2020. Antarctic Bottom Water warming in the Brazil Basin: 1990s through 2020, from WOCE to Deep Argo. *Geophys. Res. Lett.* 47:e2020GL089191

Johnson GC, Lyman JM. 2020. Warming trends increasingly dominate global ocean. *Nat. Clim. Change* 10:757-61

Johnson GC, Lyman JM, Boyer T, Cheng L, Domingues CM, et al. 2019a. Global Oceans: Ocean heat content, in the State of the Climate in 2018. *Bull. Am. Meteorol. Soc.* 100:S74-6

Johnson GC, Lyman JM, Loeb NG. 2016. Correspondence: Improving estimates of Earth's energy imbalance. *Nat. Clim. Change* 6:639-40

Johnson GC, Lyman JM, Purkey SG. 2015. Informing Deep Argo array design using Argo and full-depth hydrographic section data. *J. Atmos. Ocean. Technol.* 32:2187-98

Johnson GC, Purkey SG, Zilberman NV, Roemmich D. 2019b. Deep Argo quantifies bottom water warming rates in the southwest Pacific basin. *Geophys. Res. Lett.* 46:2662-9

Johnson GC, Schmidtko S, Lyman JM. 2012. Relative contributions of temperature and salinity to seasonal mixed layer density changes and horizontal density gradients. *J. Geophys. Res. Oceans* 117:C04015

Jones DC, Holt HJ, Meijers AJS, Shuckburgh E. 2019. Unsupervised clustering of Southern Ocean Argo float temperature profiles. *J. Geophys. Res. Oceans* 124:390-402

Katsumata K. 2016. Eddies observed by Argo Floats. Part I: Eddy transport in the upper 1000 dbar. *J. Phys. Oceanogr.* 46:3471-86

Kawai Y, Hosoda S, Uehara K, Suga T. 2021. Heat and salinity transport between the permanent pycnocline and the mixed layer due to the obduction process evaluated from a gridded Argo dataset. *J. Oceanogr.* 77:75-92

King BA, Firing E, and Joyce TM. 2001. Shipboard observations during WOCE. Chapter 3.1 in *Ocean Circulation and Climate: Observing and Modelling the Global Ocean*, ed. G Siedler, J Church, WJ Gould. International Geophysics Series, Volume 77, Academic Press

King RR, Lea DJ, Martin MJ, Mirouze I, Heming J. 2020. The impact of Argo observations in a global weakly coupled ocean–atmosphere data assimilation and short-range prediction system. *Q. J. R. Meteorol. Soc.* 146:401-14

Kolodziejczyk N, Llovel W, Portela E. 2019. Interannual variability of upper ocean water masses as inferred from Argo array. *J. Geophys. Res. Oceans* 124: 6067-85

Kumar A, Chen M, Xue Y, Behringer D. 2015. An analysis of the temporal evolution of ENSO prediction skill in the context of the equatorial Pacific Ocean observing system. *Mon. Weather Rev.* 143:3204-13

Kushnir Y, Scaife AA, Arritt R, Balsamo G, Boer G, et al. 2019. Towards operational predictions of the near-term climate. *Nat. Clim. Change* 9:94-101

Kwon YO, Riser SC. 2004. North Atlantic Subtropical Mode Water: A history of ocean-atmosphere interaction 1961-2000. *Geophys. Res. Lett.* 31:L19307

Lavender KL, Davis RE, Owens WB. 2000. Mid-depth recirculation observed in the interior Labrador and Irminger seas by direct velocity measurements. *Nature* 407:66-69

Laxenaire R, Speich S, Stegner A. 2019. Evolution of the thermohaline structure of one Agulhas ring reconstructed from satellite altimetry and Argo floats. *J. Geophys. Res. Oceans* 124:8969-9003

Laxenaire R, Speich S, Stegner A. 2020. Agulhas ring heat content and transport in the South Atlantic estimated by combining satellite altimetry and Argo profiling floats data. *J. Geophys. Res. Oceans* 125:e2019JC015511

Lea DJ, Mirouze I, Martin MJ, King RR, Hines A, et al. 2015. Assessing a new coupled data assimilation system based on the Met Office Coupled Atmosphere–Land–Ocean–Sea Ice Model. *Mon. Weather Rev.* 143:4678-94

Leuliette EW. 2015. The balancing of the sea-level budget. *Curr. Clim. Change Rep*. 1:185-91

Levitus S, Antonov J, Boyer T. 2005. Warming of the world ocean, 1955-2003. *Geophys. Res. Lett.* 32:L02604

Li G, Cheng L, Zhu J, Trenberth KE, Mann ME, Abraham JP. 2020. Increasing ocean stratification over the past half-century. *Nat. Clim. Change* 10:1116–23

Lin, I-I, Chen C-H, Pun I-F, Liu WT, Wu C-C. 2009. Warm ocean anomaly, air sea fluxes, and the rapid intensification of tropical cyclone Nargis (2008). *Geophys. Res. Lett.* 36:L03817

Lozier MS, Dave AC, Palter JB, Gerber LM, Barber RT. 2011. On the relationship between stratification and primary productivity in the North Atlantic. *Geophys. Res. Lett.* 38:L18609

Majumder S, Schmid C, Halliwell G. 2016. An observations and model-based analysis of meridional transports in the South Atlantic. *J. Geophys. Res. Oceans* 121:5622-38

Meehl GA, Goddard L, Boer G, Burgman R, Branstator G, et al. 2014. Decadal climate prediction: An update from the trenches. *Bull. Am. Meteorol. Soc.* 95:243-67

Meehl GA, Goddard L, Murphy J, Stouffer RJ, Boer G, et al. 2009. Decadal prediction: Can it be skillful? *Bull. Am. Meteorol. Soc.* 90:1467-85

Mrvaljevic RK, Black PG, Centurioni LR, Chang Y-T, D'Asaro EA, et al. 2013. Observations of the cold wake of Typhoon Fanapi (2010). *Geophys. Res. Lett.* 40:316-21

Munk W. 2003. Ocean freshening, sea level rising. *Science* 300:2041-3

Nagano A, Hasegawa T, Ueki I, Ando K. 2017. El Niño–Southern Oscillation-time scale covariation of sea surface salinity and freshwater flux in the western tropical and northern subtropical Pacific. *Geophys. Res. Lett.* 44:6895-903

Oka E, Kouketsu S, Toyama K, Uehara K, Kobayashi T, et al. 2011. Formation and subduction of central mode water based on profiling float data, 2003-08. *J. Phys. Oceanogr.* 41:113-29

Oka E, Qiu B, Takatani Y, Enyo K, Sasano D, et al. 2015. Decadal variability of Subtropical Mode Water subduction and its impact on biogeochemistry. *J. Oceanogr.* 71:389-400

Oke PR, Balmaseda MA, Benkiran M, Cummings JA, Dombrowsky E, et al. 2009. Observing system evaluations using GODAE systems. *Oceanography* 22:144-53

Olita A, Capet A, Claret M, Mahadevan A, Poulain PM, et al. 2017. Frontal dynamics boost primary production in the summer stratified Mediterranean sea. *Ocean Dyn.* 67:767-82

Oliver ECJ, Benthuysen JA, Darmaraki S, Donat MG, Hobday AJ, et al. 2021. Marine heatwaves. *Annu. Rev. Mar. Sci.* 13:313-42

Ollitrault M, Colin de Verdière A. 2014. The ocean general circulation near 1000-m depth. *J. Phys. Oceanogr.* 44:384-409

Ollitrault M, Rannou J-P. 2013. ANDRO: An Argo-based deep displacement dataset. *J. Atmos. Ocean. Technol.* 30:759-88

Park JJ, Kwon Y-O, Price JF. 2011. Argo array observation of ocean heat content changes induced by tropical cyclones in the North Pacific. *J. Geophys. Res.* 116:C12025

Pauthenet E, Roquet F, Madec G, Sallée J-B, Nerini D. 2019. The thermohaline modes of the Global Ocean. *J. Phys. Oceanogr.* 49:2535-52

Piecuch CG, Quinn KJ. 2016. El Niño, La Niña, and the global sea level budget. *Ocean Sci.* 12:1165-77

Piron A, Thierry V, Mercier H, Caniaux G. 2017. Gyre-scale deep convection in the subpolar North Atlantic Ocean during winter 2014–2015. *Geophys. Res. Lett.* 44:1439-47

Portela E, Kolodziejczyk N, Maes C, Thierry V. 2020. Interior water-mass variability in the Southern Hemisphere oceans during the last decade. *J. Phys. Oceanogr.* 50:361-81

Purkey SG, Johnson GC. 2013. Antarctic Bottom Water warming and freshening: Contributions to sea level rise, ocean freshwater budgets, and global heat gain. *J. Clim.* 26:6105-22

Qu T, Yu J-Y. 2014. ENSO indices from sea surface salinity observed by Aquarius and Argo. *J. Oceanogr.* 70:367-75

Qu T, Zhang L, Schneider N. 2016. North Atlantic subtropical underwater and its year-to-year variability in annual subduction rate during the Argo period. *J. Phys. Oceanogr.* 46:1901-16

Qu TD, Gao S, Fukumori I, Fine RA, Lindstrom EJ. 2008. Subduction of South Pacific waters. *Geophys. Res. Lett.* 35:L02610

Riser SC, Freeland HJ, Roemmich D, Wijffels S, Troisi A, et al. 2016. Fifteen years of ocean observations with the global Argo array. *Nat. Clim. Change* 6:145-53

Roach CJ, Balwada D, Speer K. 2016. Horizontal mixing in the Southern Ocean from Argo float trajectories. *J. Geophys. Res. Oceans* 121:5570-86

Roach CJ, Balwada D, Speer K. 2018. Global observations of horizontal mixing from Argo float and surface drifter trajectories. *J. Geophys. Res. Oceans* 123:4560-75

Roberts MJ, Jackson LC, Roberts CD, Meccia V, Docquier D, Koenigk T, et al. 2020. Sensitivity of the Atlantic Meridional Overturning Circulation to model resolution in CMIP6

HighResMIP simulations and implications for future changes. *J. Adv. Model. Earth Syst.* 12:e2019MS002014 https://doi.org/10.1029/2019MS002014

Robson J, Aksenov Y, Bracegirdle TJ, Dimdore-Miles O, Griffiths PT, et al. 2020. The evaluation of the North Atlantic Climate System in UKESM1 historical simulations for CMIP6. *J. Adv. Model. Earth Syst.* 12:e2020MS002126

Robson JI, Sutton RT, Smith DM. 2012. Initialized decadal predictions of the rapid warming of the North Atlantic Ocean in the mid 1990s. *Geophys. Res. Lett.* 39:L19713

Roemmich D, Gilson J. 2009. The 2004-2008 mean and annual cycle of temperature, salinity, and steric height in the global ocean from the Argo Program. *Prog. Oceanogr.* 82:81-100

Roemmich D, Gilson J. 2011. The global ocean imprint of ENSO. *Geophys. Res. Lett.* 38:L13606

Roemmich D, Gilson J, Sutton P, Zilberman N. 2016. Multidecadal change of the South Pacific Gyre circulation. *J. Phys. Oceanogr.* 46:1871-83

Roemmich D, Gould WJ, Gilson J. 2012. 135 years of global ocean warming between the Challenger expedition and the Argo Programme. *Nat. Clim. Change* 2:425-8

Roullet G, Capet X, Maze G. 2014. Global interior eddy available potential energy diagnosed from Argo floats. *Geophys. Res. Lett.* 41:1651-6

Sallee JB, Speer K, Rintoul S, Wijffels S. 2010. Southern Ocean thermocline ventilation. *J. Phys. Oceanogr.* 40:509-29

Sasaki YN, Schneider N, Maximenko N, Lebedev K. 2010. Observational evidence for propagation of decadal spiciness anomalies in the North Pacific. *Geophys. Res. Lett.* 37:L07708

Scannell HA, Johnson GC, Thompson L, Lyman JM, Riser SC. 2020. Subsurface evolution and persistence of marine heatwaves in the northeast Pacific. *Geophys. Res. Lett.* 47:e2020GL090548

Schanze JJ, Schmitt RW, Yu LL. 2010. The global oceanic freshwater cycle: A state-of-the-art quantification. *J. Mar. Res.* 68:569-95

Schmidtko S, Johnson GC, Lyman JM. 2013. MIMOC: A global monthly isopycnal upper-ocean climatology with mixed layers. *J. Geophys. Res. Oceans* 118:1658-72

Stockdale T., Alonso-Balmaseda M, Johnson S, Ferranti L, Molteni F, et al. 2018. SEAS5 and the future evolution of the long-range forecast system. ECMWF Tech. Memo. 835, European Centre for Medium Range Weather Forecasts, Berkshire, England https://doi.org/10.21957/z3e92di7y

Stommel H. 1957. Abyssal circulation of the ocean. *Nature* 180:733-4

Storto A, Alvera-Azcárate A, Balmaseda MA, Barth A, Chevallier M, et al. 2019. Ocean reanalyses: Recent advances and unsolved challenges. *Front. Mar. Sci.* 6:418

Sun B, Liu C, Wang F. 2019. Global meridional eddy heat transport inferred from Argo and altimetry observations. *Sci. Rep.* 9:1345

Thompson PR, Widlansky MJ, Leuliette E, Sweet W, Chambers DP, et al. 2020. Global Oceans: Sea level variability and change, in the State of the Climate in 2019. *Bull. Am. Meteorol. Soc.* 101:S84–S87.

Toyama K, Iwasaki A, Suga T. 2015. Interannual variation of annual subduction rate in the North Pacific estimated from a gridded Argo product. *J. Phys. Oceanogr.* 45:2276-93

Trenberth KE, Fasullo JT. 2017. Atlantic meridional heat transports computed from balancing Earth's energy locally. *Geophys. Res. Lett.* 44:1919-27

Trossman DS, Thompson L, Kelly KA, Kwon YO. 2009. Estimates of North Atlantic ventilation and mode water formation for winters 2002-06. *J. Phys. Oceanogr.* 39:2600-17

Vellinga M, Copsey D, Graham T, Milton S, Johns T. 2020. Evaluating benefits of two-way ocean-atmosphere coupling for global NWP forecasts. *Weather Forecast.* 35:2127-44

Voldoire A, Saint-Martin D, Senesi S, Decharme B, Alias A, et al. 2019. Evaluation of CMIP6 DECK experiments with CNRM-CM6-1. *J. Adv. Model. Earth Syst.* 11:2177-213

von Schuckmann K, Cheng LJ, Palmer MD, Hansen J, Tassone C, et al. 2020. Heat stored in the Earth system: where does the energy go? *Earth Syst. Sci. Data* 12:2013-41

Wang X, Bhatt V, Sun Y-J. 2015. Seasonal and inter-annual variability of western subtropical mode water in the South Pacific Ocean. *Ocean Dyn.* 65:143-54

Warren, B. 1981. Deep circulation of the world ocean. In *Evolution of Physical Oceanography: Scientific Surveys in Honor of Henry Stommel*, ed. BA Warren and C Wunsch, pp. 6-41. Cambridge: MIT Press.

Whalen CB, MacKinnon JA, Talley LD, Waterhouse AF. 2015. Estimating the mean diapycnal mixing using a finescale strain parameterization. *J. Phys. Oceanogr.* 45:1174-88

Wijffels S, Roemmich D, Monselesan D, Church J, Gilson J. 2016. Ocean temperatures chronicle the ongoing warming of Earth. *Nat. Clim. Change* 6:116-8

Willis JK. 2010. Can in situ floats and satellite altimeters detect long-term changes in Atlantic Ocean overturning? *Geophys. Res. Lett.* 37:L06602

Wong APS, Wijffels SE, Riser SC, Pouliquen S, Hosoda S, et al. 2020. Argo Data 1999-2019: Two million temperature-salinity profiles and subsurface velocity observations from a global array of profiling floats. *Front. Mar. Sci.* 7:700

Woolnough SJ, Vitart F, Balmaseda MA. 2007. The role of the ocean in the Madden-Julian Oscillation: Implications for MJO prediction. *Q. J. R. Meteorol. Soc.* 133:117-28

Wyville Thompson, C. and Murray, C. 1885. *The voyage of the HMS Challenger 1873-1876*. Narrative Vol. 1. Johnson Reprint Corp. Available at https://archimer.ifremer.fr/doc/00000/4751

Yang J, Riser SC, Nystuen JA, Asher WE, Jessup AT. 2015. Regional rainfall measurements using the Passive Aquatic Listnere during the SPURS field campaign. *Oceanography* 28:124-33

Yeager S, Karspeck A, Danabasoglu G, Tribbia J, Teng HY. 2012. A decadal prediction case study: Late twentieth-century North Atlantic Ocean heat content. *J. Clim.* 25:5173-89

Zanowski H, Johnson GC, Lyman JM. 2019. Equatorial Pacific 1,000-dbar velocity and isotherm displacements from Argo data: Beyond the mean and seasonal cycle. *J. Geophys. Res. Oceans* 124:7873-82

Zhang S, Liu Z, Zhang X, Wu X, Han G, et al. 2020. Coupled data assimilation and parameter estimation in coupled ocean-atmosphere models: a review. *Clim. Dyn.* 54:5127-44

Zhang Z, Wang W, Qiu B. 2014. Oceanic mass transport by mesoscale eddies. *Science* 345:322-4

Zhang ZG, Zhang Y, Wang W, Huang RX. 2013. Universal structure of mesoscale eddies in the ocean. *Geophys. Res. Lett.* 40:3677-81

Zhao M, Hendon HH, Alves O, Liu G, Wang G. 2016. Weakened Eastern Pacific El Nino predictability in the early twenty-first century. *J. Clim.* 29:6805-22

ZhuY, Zhang R, Sun J. 2020. North Pacific upper-ocean cold temperature biases in CMIP6 simulations and the role of regional vertical mixing. *J. Clim.* 33(17):7523-38

Zilberman NV, Roemmich DH, Gille ST. 2014. Meridional volume transport in the South Pacific: Mean and SAM-related variability. *J. Geophys. Res. Oceans* 119:2658-78

Zuo H, Balmaseda MA, Tietsche S, Mogensen K, Mayer M. 2019. The ECMWF operational ensemble reanalysis–analysis system for ocean and sea ice: a description of the system and assessment. *Ocean Sci.* 15:779-808